
Origin theories for the eccentricities of extrasolar planets

Fathi Namouni¹

CNRS, Observatoire de la Côte d’Azur, BP 4229, 06304 Nice, France
 namouni@obs-nice.fr

1 Introduction

Planetary science has known a revolution in the year 1992 when Wolszczan and Frail discovered the first extrasolar planets around a pulsar [69]. This discovery was soon followed in 1995 by the first Jupiter-like planet around the sun-like star 51 Pegasi [41]. As of this writing we have entered the stage of statistics as more than 200 extrasolar planets are known to orbit sun-like stars. The revolution that was triggered by these discoveries changed the paradigm of what we think of as a planetary system and what we believe to be the scenarios that led up to the formation of planets. The planet around 51 Pegasi is the prototype of what has become to be known as hot Jupiters: planets with masses comparable to Jupiter’s but with periods of a few days and orbits smaller than the tenth of Mercury’s distance to the sun. Planetary orbits also seem to be eccentric. This observation is not surprising since the solar system planets have eccentric orbits except that half the extrasolar planets have eccentricities larger than 0.3 which is much more significant than Jupiter’s 0.05. Such large eccentricities are reminiscent of the small body populations of the solar system that got stirred up by their gravitational interactions with the larger planets. In this respect, extrasolar planetary eccentricities are more unusual, witness the median eccentricity of 0.13 of main belt asteroids larger than 50 km. The planetary revolution did not stop at orbital radii and eccentricities: 10% of known planetary systems belong to binary star systems and only one planet so far is in a triple stellar system. Multiple planets around a single star make up about 10% of known planets.

In essence, the planetary revolution heralded the coming of a new planetary principle: orbital diversity is a rule of planetary formation. Diversity here is not meant to imply subtle changes but drastic ones with respect to the aspect of the solar system. This state of affairs has prompted a serious revision of the theories of planetary formation: hot Jupiters with few-day orbits could not have formed in situ. Instead they have formed outside a few AU for a sun-like star where it is possible for ices to condense and for the planets to capture

large amount of gas from the protoplanetary disk. Only after they formed, did they travel all the way to meet their current orbits. It is interesting to note that the concept of radial migration was already known in the contexts of accretion disks [32] in binary star systems and of planetary rings [18]. Only before 1995, one could not plausibly contemplate the prospect of suggesting the existence of massive planets that traveled all the way from Jupiter's current location just to stop on a close orbit with a few-day period. The basic aspects of the process of planetary migration through the tidal interaction of a planet with the gaseous protoplanetary disk are now well understood [65] yet an important challenge remains: what stops planetary migration towards the star? The leading contender for stopping planetary migration is the planet's interaction with the stellar magnetosphere but a definitive quantitative description is still lacking.

Extrasolar planetary eccentricities have equally resulted in a drastic change of perception: it is often heard that it is not the extrasolar planets that are eccentric, rather it is the solar system that lacks eccentricity. This perception is encouraged by the availability of some simple instabilities that one can set up in a many-body gravitational system to simulate the generation of the wild orbits of extrasolar planets. Upon close examination such instabilities as well as other eccentricity scenarios do not tell the whole story of how extrasolar planets become eccentric. In fact, just as the features of the planetary migration process yield constraints on the planetary formation scenarios, so do the various theories of the eccentricity excitation.

It is the aim of this chapter to review the various processes of the origin of extrasolar planets' eccentricities in the context of planetary formation. We start by reviewing the properties of extrasolar planetary orbits in section 2. Section 3 contains a commentary on the various known theories of eccentricity excitation. Section 4 specializes in a recent addition to the eccentricity theories based on an relationship between the planets and the stellar jet that is powered by the protoplanetary accretion disk. The final section 5 discusses how the eccentricity origin problem may contribute further to the theory of planet formation.

2 Eccentricity observations

Extrasolar planets are detected with various observational techniques [55]. The Doppler analysis of the reflex velocity of the host star is by far the most successful technique to date. It is also the technique that has uncovered the large eccentricities of extrasolar planets. If a planet has a circular orbit, the analyzed stellar spectrum yields a sinusoidal oscillation of the stellar reflex motion. If the planet is on an eccentric orbit, the reflex motion as a function of time becomes distorted with respect to a pure sine reflecting the unequal times the star spends in different locations along its orbit around the center of mass of the star-planet system (Figure 1). The discovery of large eccentricity

orbits by the Doppler reflex velocity method is due to its ability to detect planets on wider orbits in contrast to that to the transit method. Planets on many-day periods have usually undergone tidal circularization by the host star.

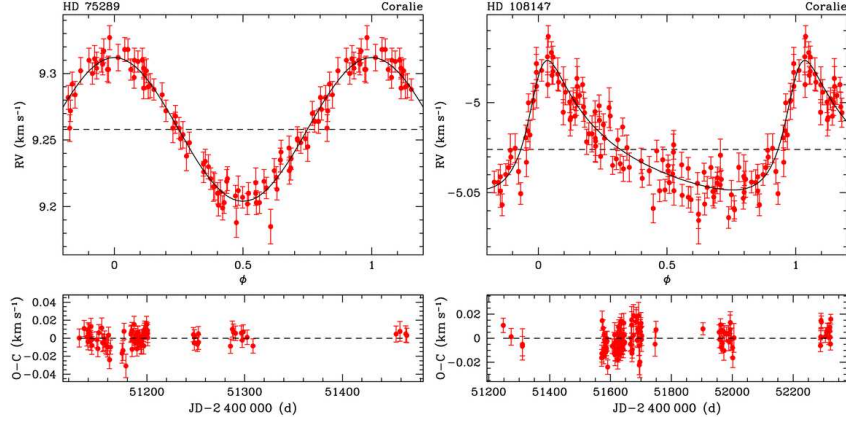


Fig. 1. Reflex velocity of the stars HD 75289 (left) [63] and HD 108147 (right) [51]. The planet around HD 75289 has a circular orbit while that around HD 108147 has an orbital eccentricity of 0.5. Pictures taken from the Geneva Extrasolar Planet Search <http://obswww.unige.ch/~udry/planet/planet.html>

The statistical analysis of extrasolar planet eccentricities reveals very few clues as to the origin of the elongated orbits. For the known sample of 196 planets discovered by the reflex velocity and transit techniques, the median eccentricity is at 0.21 if all planets are counted and at 0.28 if planets with periods smaller than 5 days are excluded because their circular orbits simply reflect tidal circularization. The prevalence of such large eccentricities and the large typical mass of the detected planets (comparable to Jupiter's) has encouraged the comparison of the extrasolar planetary systems to binary star systems. Depending on the methods used, similarities in the eccentricity distribution of both populations can be found [57] or not [21]. What is agreed upon is that there is no correlation between the size of the orbits and their eccentricities in each population, and no striking resemblance of the scatter of both populations in an orbital size versus eccentricity plane. The size of the orbit usually refers to either the semi-major axis or the pericentre radius. The latter is used to account for those orbits that have not yet had enough time to be circularized –as the pericentre distance is conserved under stellar tides. Finally, eccentricities show a vague correlation with the planetary masses with heavier planets enjoying larger eccentricities.

3 Eccentricity origin theories

Seven known explanations have been put forward to account for the large eccentricities of extrasolar planets. They are: (1) planet-planet scattering, (2) planet-protoplanetary disk interaction, (3) Kozai’s secular cycles, (4) excitation through radial migration into a mean motion resonance, (5) Stellar encounters, (6) stellar-like N-body relaxation, and (7) excitation through stellar jet acceleration. In the following, we comment on these possibilities by discussing their instability types, characteristic timescales, their epoch of applicability as well as their advantages and drawbacks.

3.1 Planet-planet scattering

Planet-planet scattering is a simple process to generate eccentric orbits in an N-body gravitational system. If a system of two or more planets on planar circular orbits find themselves “initially” closer than is permitted by Chirikov’s criterion for the overlapping of mean motion resonances [68], the planets scatter off one another leading to a system with more stable albeit eccentric configurations. Depending on the number, masses and “initial” spacings of the planets, the instability timescale varies between 10^3 to 10^7 years [52, 67, 15, 40, 16]. The epoch that is referred to by the adjective “initial” is that of the disappearance of the agent or the conditions that kept the planets from scattering off one another in the first place. This epoch is customarily associated with a significant dispersal of the parent gaseous protoplanetary disk. As well shall point out in the next section, planet-disk interaction is known to primarily erase orbital eccentricities. An additional condition for planet-planet scattering to be operational is the absence of a significant population of smaller bodies such as the primordial asteroid belt. Depending on the mass spectrum in the planetary system, the smaller populations are able to limit the growth of the planetary eccentricities through dynamical friction [4]. This at least how it is believed that the terrestrial planets in the solar system did not acquire large eccentricities [1, 44]. Numerical works that tackle the extrasolar eccentricity problem using planet-planet scattering do not consider the effect of leftover small-body populations after the gaseous disk has dispersed. Planets are set up at a few Hill radii from one another and initial conditions are sampled to reproduce the eccentricity of certain observed systems. The general excitation trend of planet-planet scattering leads to larger eccentricities than the ones observed. What may prove to be a serious problem for planet-planet scattering is the eccentricity distribution obtained in multiple systems that contain Jupiter-mass planets as well as Earth-mass planets. The conservation of angular momentum in this case will force the much smaller planets to have much larger eccentricities than the Jovian planets.

3.2 Planet-disk interaction

A planet embedded in a gaseous disk excites sound waves at the locations of its mean motion resonances within the disk akin to the gravity waves excited by Saturn’s satellites in its ring system. The density enhancements at the mean motion resonances act back on the planet resulting in gravitational torque. Two types of resonances contribute to this torque: (1) corotation resonances that primarily affect the semi-major axis and tend to damp any acquired eccentricity and (2) Lindblad resonances that primarily affect the eccentricity and tend to increase it [17, 18]. The torque contribution of the former is larger than the latter’s by about 5%. At first sight, planet-disk interaction damps the eccentricity on timescale that depends strongly on the disk’s thickness and less strongly on the disk’s mass density and the planet’s mass [64, 2, 37]. The torques originating from higher order resonances as well as those pertaining to the relative inclination of the planet and the disk do not change the outcome significantly [19, 45]. Only if the corotation torque saturates, can the Lindblad resonances increase the eccentricity [19, 20]. The conditions under which saturation arises are difficult to quantify explaining why an eccentricity increase due to a disk-planet interaction has never been observed in numerical simulations although this might be due to numerical artefacts [38].

3.3 Secular Kozai cycles

In his study of asteroids perturbed by Jupiter on high eccentricity and inclination orbits, Kozai [28] showed that the averaging of the interaction potential over the mean motion without expanding the force amplitude in terms of eccentricity and inclination leads to new types of secular resonances. The conservation of the vertical component of angular momentum (vertical refers to the direction of Jupiter’s orbital normal) shows that when the orbital eccentricity increases, the inclination decreases. In particular, if objects are set up on inclined but circular orbits, large eccentricities can be achieved as the inclination decreases in its motion around the secular resonance cycle. The application of the Kozai cycle to the eccentricities of extrasolar planets assumes that there is a binary star on a not-too-far inclined orbit that perturbs the planet that formed in a circular orbit in a timescale shorter than the Kozai libration cycle. In essence, the secular Kozai cycle idea transforms the eccentricity problem into an inclination problem. In this sense, the observed planets do not possess a proper eccentricity but one that is forced by the stellar binary and that will always oscillate between its original value, zero, and a maximum value depending on the planetary-binary semi-major axis ratio, the binary’s mass and its orbital inclination with respect to the plane on which the planet initially formed. When applied to specific binary star systems with one planet, the Kozai mechanism works fine and helps characterize the orbit and mass of the secondary star required to excite eccentricity [27, 42, 14]. Statistically, Kozai based excitation of one-planet binary systems tend to yield

larger eccentricities than observed [58]. As T Tauri stars form in multiple systems, it is not unreasonable to try and apply the Kozai mechanism to the whole sample of observed extrasolar planets. The problem is that the Kozai cycle is usually destroyed by mutual gravitational interactions. The addition of more planets to the one-planet binary system, forces the precession of the planets' pericentres. If the planets are of comparable mass as it is observed in multiplanet systems, the Kozai cycle is lost.

3.4 Mean-motion resonances

The role of mean motion resonances in exciting orbital eccentricity has its roots in the study of the orbital evolution of Jupiter's and Saturn's regular satellites under planetary and satellite tides [50]. These satellite systems are known to be in or to have crossed mean motion resonances thereby acquiring forced eccentricities. The combined modeling of the orbital evolution, capture into resonance and the tidal interaction lends valuable bounds on the dissipation factors of Jupiter, Saturn and their satellites. Extrasolar planets form in a gaseous disk that does not dissipate after they acquired most of their masses or else hot Jupiters would not exist. Planet-disk interaction naturally gives rise to orbital migration with different planets in the same system migrating at different rates. This differential migration makes planets in the same system encounter mean motion resonances. Capture into resonance may occur depending on whether the migration is convergent or divergent (for instance if the outer planet is moving faster or slower than the inner planet). Convergent migration leads to capture into resonance. The subsequent common migration of a planetary pair in resonance pumps up the eccentricities on the migration timescale [31, 70]. Divergent migration does not lead to resonance capture, instead eccentricity jumps are acquired at resonance passage [7, 62]. While convergent migration is certainly the way the known resonant multiple systems have acquired their eccentricities, this excitation method involves a mystery that may shed light on how to halt planet migration in a gas disk. The mystery consists of the observation that convergent migration is far too efficient in exciting eccentricities to the point where in many systems, when capture occurs, migration must stop quickly thereafter or else eccentricities are pumped up to much larger values than those observed. As it is implausible to invoke the dispersal of the gas disk, planetary migration may become ineffective because of the nonlinear response of the gas disk to the planet pair. It is interesting to note that when capture occurs, the planetary relative inclinations may be excited as unlike planetary satellites that orbit Jupiter and Saturn, the central potential is keplerian. Consequently, for the same order, eccentricity and inclination resonances are close (but not coincident as the gas disk modifies the pericentre and node precession rates). Planet-disk interaction is not well understood for large eccentricity planets and off-plane (inclined with respect to the disk) orbits. The often used formulas for eccentricity damping from the disk torques have not been verified for eccentric and

inclined planets. Divergent migration has the advantage of being applicable to the wider non-resonant multiplanet systems. For a planetary pair, divergent migration requires that the inner planet migrates faster than the outer one. Gap driven migration (also known as type II) is favorable to such a condition as the migration rate is the viscous timescale of the disk. Divergent migration may take place because viscosity is likely to be a decreasing function of the distance to the star. If however the part of the disk that is located between the two planets is dispersed as when the two planetary gaps merge, the direction and rate of migration may be altered significantly [39].

3.5 Stellar encounters

Stellar encounters are common events in star clusters. A planetary system that encounters a star will have its planets feel a tidal force that elongates their orbits. For inner planets that orbit close to the host star, the excitation which lasts for about 1000 years will occur on a secular timescale. Outer planets if they exist will feel a localized impulse somewhere in their orbits. Typical encounter frequencies are of one in 5×10^9 years while typical encounter parameters are a few hundred AU. Unless planets are way outside the classical planetary region (inside 30 AU), excitation is not efficient [71]. To reverse this conclusion and account for the eccentricities of inner planets, the system must contain several planets with increasing distance and mass from the star in order propagate the stellar tug felt by the outermost planet down to the innermost ones [71].

3.6 Stellar-like relaxation

The qualitative similarity of the eccentricities of extrasolar planets and stellar binaries suggests that planets may form through similar processes as those of multiple stellar systems. If planets formed by gravitational instability, the formation time is so short that the planets find themselves confined to a smaller space than their orbital stability permits. The relaxation of such systems leads to some planetary ejections and many large eccentricity orbits [49]. The applicability of this scenario is limited by two facts: first, the minimum planet mass the gravitational instability allows is a few Jupiter masses. This means that stellar-like relaxation does not work for planets with masses comparable to or smaller than Jupiter's. Second, if a two-phase formation where small planets form through rocky core accretion and the larger ones through gravitational instability [60], then it is likely that the relaxation of the larger planets destroys the smaller planets. This is because the gravitational instability timescales are usually smaller than the planetesimal accumulation timescales. In fact, if large mass planets form through gravitational instability, they are likely to inhibit planetesimal accumulation by clearing the inner disk before planetary embryos are born.

4 Jet-induced excitation

Stellar jets enter the eccentricity excitation problem because of their ubiquity and simplicity [46]. The story of how this works is as follows: although there is disagreement on whether there is a statistically significant resemblance between the eccentricity distributions of extrasolar planets and stellar binary systems, the qualitative similarity is beyond doubt. Those who wish for the similarity to be quantitative, would like to affirm the view that planets are the lower end of the outcome of star formation. This question has been settled observationally in 2005 with two observations: the first is a hot Saturn with a giant rocky core discovered by combining the Doppler reflex velocity method with transit photometry [54]. The second is the imaging of the first planetary candidate which because of bias due to contrast and resolution happens to be a warm distant companion orbiting a young brown dwarf [5]. This proves that planets do not need large rocky cores and may form by gravitational instability. Exit the link between how planets form and their eccentricities.

If planets do not form like binary stars, perhaps they undergo similar excitation processes that lend them similarly elongated orbits. In view of the different physical environments where planets and stars form, the simplest possible excitation process may depend weakly or not at all on the local dynamics of the stellar or planetary companion. Mathematically, this amounts to saying that the acceleration imparted by the process is independent of position and velocity.

Simplicity therefore dictates that the process imparts a constant acceleration that operates during a finite time window. Simplicity also comes with two added advantages: we can already know the excitation time scale and the minimal acceleration amplitude. Dimensional analysis shows that the excitation timescale has to be proportional to v/A where v is the keplerian velocity of the companion around the main star. Further, if the acceleration is to achieve its purpose within the lifetime of the system, v/A must be smaller than about 10^9 years. This tells us that the acceleration $A > 3 \times 10^{-16} (v/10 \text{ km s}^{-1}) \text{ km s}^{-2}$.

The process lacks one more attribute: direction. If the acceleration is independent of the formation processes, its direction cannot depend on anything related to the planetary companion such as its orbital plane or the direction from the star to the companion. In an inertial frame related to the planetary or stellar system, we are not left with much choice but the star's rotation axis.

To sum up, what we are looking for is a process that appears everywhere where planet and star formation takes place, acts like a rocket (i.e. with an acceleration that does not depend on the position and velocity of the system) and whose direction is related to the star's rotation axis. The answer is stellar jets [12, 23].

Do planets exist when jets are active? The answer is quite likely. Known hot Jupiters have moved close to their host stars because of their interaction with the gas disk. So we know the gas disk was present and had viscosity well after planets finished forming. The gas accreting on the star because of viscosity

is the main ingredient along with the magnetic field that threads it needed to launch stellar jets and disk winds. It would therefore be an interesting coincidence that jets shut off when planets appear in the gas disk a few AU away from the star well outside the jet launching region.

Are there any observational hints that jet-sustaining disks contain planets? The only possible hint so far is the observation of variable brightness asymmetries in some jet-sustaining disks [8, 56, 66]. The variability timescales of a few days to a few years are so small that they imply either a peculiar stellar activity in the form of single hot spots or the presence of distortions in the disk at the location where the orbital period matches the variability timescale. The first option requires a complex stellar magnetic field that differentiates strongly between the two stellar poles. The second option may be caused distortions in the disk whose origin could be the presence of embedded compact objects.

Do jets have enough strength to build eccentricity? Inferred mass loss rates for known young T Tauri stars lie in the range $\sim 10^{-8} M_{\odot} \text{ year}^{-1}$ to $10^{-10} M_{\odot} \text{ year}^{-1}$ and may be two orders of magnitude larger depending on the way the rate is measured from the luminosity of forbidden lines [22, 25, 29]. The jet also needs to be asymmetric with respect to the star's equator plane or else there would be no acceleration. Interestingly, a growing number of bipolar jets from young stars [24, 13, 30, 35] are known to be asymmetric as the velocities of the jet and counterjet differ by about a factor of 2. Mass loss processes in young stars therefore yield accelerations:

$$A \sim 10^{-13} \left(\frac{\dot{M}}{10^{-8} M_{\odot} \text{ year}^{-1}} \right) \left(\frac{v_e}{300 \text{ km s}^{-1}} \right) \left(\frac{M_{\odot}}{M} \right) \text{ km s}^{-2}. \quad (1)$$

where M is the stellar mass and v_e is the outflow's high velocity component. As jets are time-variable processes, the above estimate is only indicative of the epochs at which the rates and velocities are measured. In this sense, it is closer to being a lower bound on what accelerations really are over the jet's lifetime. What is clear is that asymmetric jet acceleration is larger than the minimum amplitude of $10^{-16} (v/10 \text{ km s}^{-1}) \text{ km s}^{-2}$.

For how long can a jet operate? Jet-induced acceleration is technically no different from attaching a rocket to the star and accelerating it very slowly with respect to the outer part of the disk and the planets. As a result, the star acquires a residual velocity that must be smaller than its orbital velocity in the Galaxy or else the star is ejected. In fact, there is an even a stronger constraint on the residual velocity from the velocity dispersion in the Galaxy. Stars do not have exactly circular orbits in the Galaxy. Their motion is slightly distorted or eccentric and such eccentricity is measured as a departure of the galactic orbital velocity from that of circular motion. This velocity dispersion is known for various stellar populations and is of order a few tens of kilometers per second. Since the residual velocity imparted by the jet, V is given by the product $A\tau$ where τ is the duration of acceleration, imposing that $V < \langle v_g \rangle$

where $\langle v_g \rangle$ is the velocity dispersion in the Galaxy yields:

$$\tau \leq 10^5 \frac{3 \times 10^{-12} \text{ km s}^{-2}}{A} \frac{\langle v_g \rangle}{10 \text{ km s}^{-1}} \text{ years.} \quad (2)$$

This timescale is shorter than the disk's lifetime. In practice, we shall see that shorter times are needed.

Further excitation properties can be deduced by analyzing the effect of the combined jet-induced acceleration and the star's gravitational attraction. As the star's pull decreases with distance, there is a specific location where the latter matches the jet-induced acceleration (that is independent of position and velocity). Outside this radius, the star's pull is weak and orbits escape its gravity. This reveals an interesting feature of jet-induced acceleration: stellar jets are responsible for the outer truncation of circumstellar disks. It is clear that in the interior vicinity of the truncation radius, the orbital perturbations are large as the excitation time becomes comparable to the orbital period. In this region, the keplerian orbits are subject to a sudden excitation; not only the eccentricities are excited but the semi-major axes are also affected leading to inward or outward migration. Well inside the truncation radius, the excitation time is much larger than the orbital period. In this region, eccentricity builds up slowly over a large number of revolutions of the planet around the star and the mean orbital radius remains constant on average. Excitation in this region occurs on secular timescales. Planetary companions mostly fall inside the secular region as they are far inside the truncation radius which is more or less the size of the protoplanetary disk.

4.1 Secular jet-induced excitation

In the secular region where the excitation time is larger than the orbital period, the dynamics of excitation can be simplified by averaging the acceleration over the orbital period of the companion. For a constant acceleration, the interaction potential is simply $R = \mathbf{A} \cdot \mathbf{x}$ where \mathbf{x} is the position vector. Averaging the interaction potential amounts to averaging the position vector of a pure keplerian motion. A simple calculation shows that $\langle \mathbf{x} \rangle = -3ae \mathbf{x}(f = 0)/2r$ where f , a , e and r are the true anomaly, the semi-major axis, the eccentricity and radius of the keplerian orbit. The direction of \mathbf{x} at pericentre is that of the eccentricity vector $\mathbf{e} = \mathbf{v} \times \mathbf{h}/G(m + M) - \mathbf{x}/|\mathbf{x}|$ where \mathbf{v} is the velocity vector of the companion, G is the gravitational constant, m and M are the masses of the companion and the host star and $\mathbf{h} = \mathbf{x} \times \mathbf{v}$ is the specific angular momentum. This enables us to write the secular potential as:

$$\langle R \rangle = -\frac{3}{2}a \mathbf{A} \cdot \mathbf{e} = -\frac{3}{2}Aae \sin(\varpi - \Omega) \sin I, \quad (3)$$

where in the last equality, the z -direction of the reference frame is chosen along \mathbf{A} and ϖ , Ω , I , are the longitude of pericentre, longitude of ascending

node and the inclination of the orbit. To simplify the excitation problem further, we use the conservation of the component of angular momentum \mathbf{h} along the direction of acceleration as $\mathbf{A} \cdot \dot{\mathbf{h}} = \mathbf{A} \cdot (\mathbf{x} \times \mathbf{A}) = 0$. In the reference frame where \mathbf{A} is along the z -direction, the conservation of angular momentum yields $(1-e^2)^{1/2} \cos I = \cos I_0$ where I_0 is the initial inclination of the keplerian orbit with respect to the jet-induced acceleration. This relation enables us to eliminate the inclination variable in $\langle R \rangle$ and reduce the problem to an integrable, one dimensional system with:

$$\langle R \rangle = -\frac{3}{2} A a \sqrt{\frac{\sin^2 I_0 - e^2}{1 - e^2}} e \sin \omega. \quad (4)$$

where $\omega = \varpi - \Omega$ is the argument of pericentre. The time evolution of eccentricity and argument of pericentre is obtained from:

$$\dot{e} = -\frac{\sqrt{1-e^2}}{na^2 e} \frac{\partial \langle R \rangle}{\partial \omega}, \quad \dot{\omega} = \frac{\sqrt{1-e^2}}{na^2 e} \frac{\partial \langle R \rangle}{\partial e}, \quad (5)$$

where $n = \sqrt{G(M+m)/a^3}$ is the companion's mean motion. In this one-dimensional system, e and ω follow curves of constant $\langle R \rangle$ shown in Figure (2). There are equilibria at $\omega = \pm 90^\circ$ and $e = \sqrt{2} \sin(I_0/2)$ corresponding to $I = \cos^{-1}(\sqrt{\cos I_0})$. The maximum value of e is $\sin I_0$ and corresponds to the cycle of initially circular orbits. For these orbits, $\langle R \rangle = 0$ throughout their cycle implying that the orbits orientation can take only one value $\omega = 0$ modulo 180° .

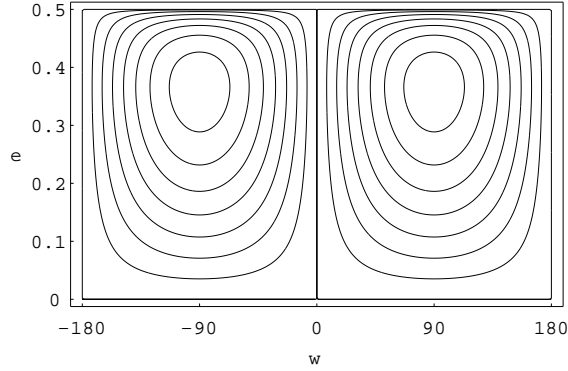


Fig. 2. Contour plots of the acceleration potential (4) in the eccentricity e and argument of pericentre $\omega(^{\circ})$ plane. The direction of acceleration makes an angle $I_0 = 30^\circ$ with respect to the companion's angular momentum vector. The time evolution of the two orbits ($e = 0, \omega = 0$) and ($e = 0.3, \omega = 90^\circ$) is shown in Figure (3).

For time-dependent accelerations and provided that the variation timescale is longer than the orbital period, the eccentricity evolution is given by:

$$\dot{e} = \frac{3A(t)\epsilon}{2na} \sqrt{\sin^2 I_0 - e^2}, \quad (6)$$

where ϵ is the sign of $\cos \omega$ which is set by the requirement that $e \geq 0$. The solution of (6) can be found exactly as:

$$e(T) = \left| \sin \left[\frac{3}{2na} \int_{-\infty}^T A(t) dt \right] \sin I_0 \right|. \quad (7)$$

The inclination is obtained from $\cos I = \cos I_0 / \sqrt{1 - e(T)^2}$. For strictly constant accelerations (infinite time window), $A(t) = A_0$ and e oscillates between 0 and $\sin I_0$ at the excitation frequency:

$$n_A = \frac{3|A_0|}{na}. \quad (8)$$

Examples of such oscillations that were obtained from the direct integration of the full equations of motion are shown in Figure (3). The good agreement between the secular solution and the results of the numerical integration comes from the fact that A is independent of position and velocity.

To optimize the excitation of a finite eccentricity from an initially circular state, the duration of acceleration needs to be smaller than half the oscillation period: $\tau < \pi na / 3|A_0|$. Examples of eccentricity excitation at three different semi-major axes (i.e. three different excitation frequencies) are shown in Figure 4. The dependence of the excitation amplitude on the ratio of the duration to the excitation time is also seen in the same Figure. Note that because eccentricity excitation in the secular region is a slow process compared to the orbital time, the convolution of the dynamics under the constant acceleration A with a finite time window has the effect of shutting off the excitation at some eccentricity value depending on the duration.

The secular excitation through jet-induced acceleration is therefore able to make e reach $\sin I_0$ and is largest if the initial orbital plane contains the direction of acceleration ($I_0 = 90^\circ$). As $\langle R \rangle = 0$ for initially circular orbits, ω and Ω , remain at zero. This forcing of the pericentre to be perpendicular to the direction of acceleration favors apsidal alignment in multiplanet system.

If the jet's inclination with respect to the companion's orbital plane is small $I_0 \ll 1$, the maximum eccentricity will be negligible. The $\sin I_0$ limitation is problematic because it is not reasonable to expect stellar jets to be highly inclined with respect to the gas disk where the companions form. Fortunately for the jet-induced excitation theory, there is a natural way out. Jets are known to precess over timescales from 10^2 to 10^4 years [10, 11, 59]. The origin of such precession is not known as we lack resolution to probe inside the jet launching region. It is possible that precession is caused by a warp in the

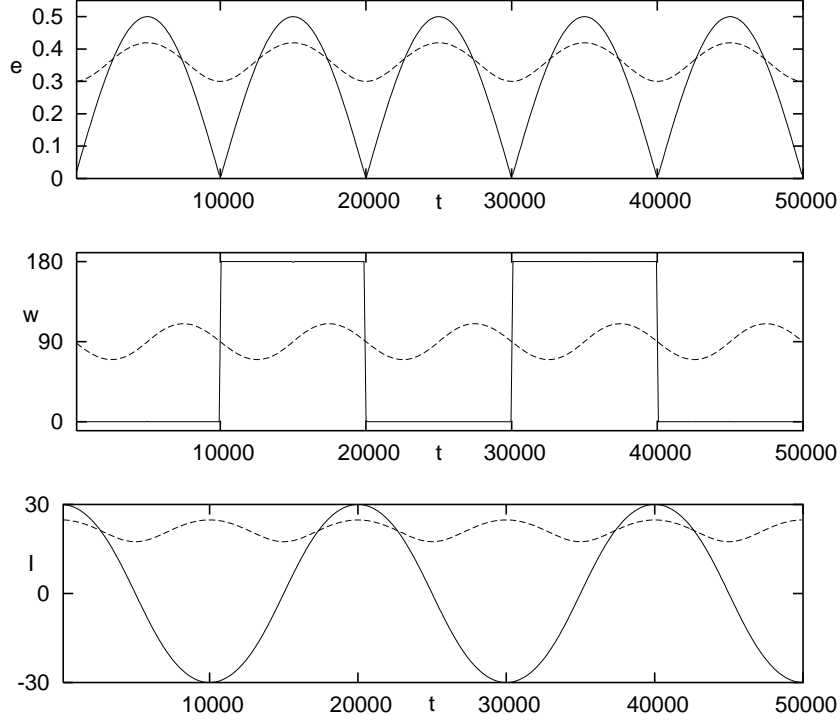


Fig. 3. Time evolution under a conservative acceleration. The eccentricity e , argument of pericentre $\omega(^{\circ})$ and inclination $I(^{\circ})$ are shown for an initially circular orbit $e = 0$ (solid) and an orbit librating about the secular resonance $\omega = 90^{\circ}$ with an initial eccentricity $e = 0.3$ (dashed). The semi-major axis is identical for both orbits and is set to unity. The acceleration corresponds to a period of 10^4 years at 1 AU. The plots were obtained by the numerical integration of the full equations of motion.

disk's plane resulting from interactions with stellar companions as T Tauri stars are known to form in multiple systems. Precession is attractive because it offers the possibility of resonance if the excitation frequency n_A matches the jet precession frequency Ω_A . This in fact is exactly what happens when the eccentricity evolution is derived in the situation where the constant magnitude acceleration rotates at a constant rate. It turns out that the corresponding secular problem is also integrable. The eccentricity and inclination evolution are given by [46]:

$$e^2 = \frac{p^2 \sin^2 \alpha}{4\nu_+^2 \nu_-^2} \left[2(3 + p^2) - 4(1 + p \cos \alpha) \cos \nu_+ t - 4(1 - p \cos \alpha) \cos \nu_- t \right. \\ \left. + (1 - p^2 + \nu_+ \nu_-) \cos(\nu_+ - \nu_-)t + (1 - p^2 - \nu_+ \nu_-) \cos(\nu_+ + \nu_-)t \right] \quad (9)$$

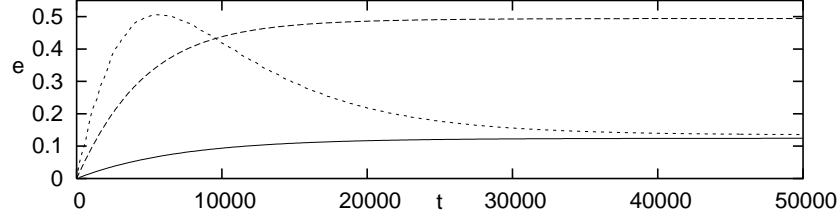


Fig. 4. Eccentricity excitation by time-dependent constant-direction accelerations. The equations of motion are integrated numerically with an acceleration $A(t) = A_0 H(t) \exp(-t/\tau)$ where $H(t)$ is the Heaviside unit step function and $A_0 = 2.21 \times 10^{-11} \text{ km s}^{-2}$. The oscillation period at 1 AU is 1.11×10^5 years. The timescale $\tau = 7200$ is chosen so that $V = 5 \text{ km s}^{-1}$. The curves correspond the semi-major axes: 1 AU (solid), 32 AU (dashed) and 128 AU (dotted).

$$\cos I = \frac{1}{2\nu_+^2 \nu_-^2 \sqrt{1-e^2}} [(p^4 - p^2 + 2 + p^2[p^2 - 3] \cos 2\alpha) + p^2 \sin^2 \alpha (p^2 + 1 + 2p \cos \alpha) \cos \nu_+ t + p^2 \sin^2 \alpha (p^2 + 1 - 2p \cos \alpha) \cos \nu_- t] \quad (10)$$

$$+ p^2 \sin^2 \alpha (p^2 + 1 - 2p \cos \alpha) \cos \nu_- t] \quad (11)$$

where α is the jet angle with respect to the z -axis of the reference frame, $\nu_{\pm}^2 = p^2 + 1 \mp 2p \cos \alpha$, $p = n_A/2\Omega_A$, and the time t is normalized by Ω_A . The companion's initial orbit is circular and lies in the xy -plane.

Nominal resonance is defined where the frequency match, $p = 1$, occurs. It corresponds to a nominal resonant semi-major axis a_{res} given as:

$$a_{\text{res}} \simeq 4 \left(\frac{M+m}{M_{\odot}} \right) \left(\frac{A}{2 \times 10^{-10} \text{ km s}^{-2}} \right)^{-2} \left(\frac{T_{\text{prec}}}{10^4 \text{ years}} \right)^{-2} \text{ AU}, \quad (12)$$

where $T_{\text{prec}} = 2\pi/\Omega_A$. In terms of the resonant semi-major axis, the frequency ratio can be written as $p = \sqrt{a/a_{\text{res}}}$. Far inside resonance ($p \ll 1$), the jet precesses faster than the eccentricity excitation leading to a reduction of the eccentricity amplitude from $\sin \alpha$ to $2p \sin \alpha$. Far outside resonance ($p \gg 1$), the jet's precession is slow compared to the eccentricity excitation so that the latter is described by a constant acceleration without rotation. In the resonance region, the proximity of p to unity increases the denominators of the eccentricity expression (9) which leads to eccentricities close to unity. At exact resonance, the eccentricity reaches unity regardless of the jet angle. The width of the region around resonance increases with the jet angle α . These features are illustrated in Figures (5) where we plot the expressions (9) and (11) for a jet angle $\alpha = 1^\circ$, an excitation time $2\pi/n_A = 10^4$ years, and the three values of p : 0.05, 0.9, and 1. Finally, we note that as the eccentricity excitation time is n_A , no resonant forcing occurs when $\Omega_A = n$ in the secular region ($n_A \ll n$).

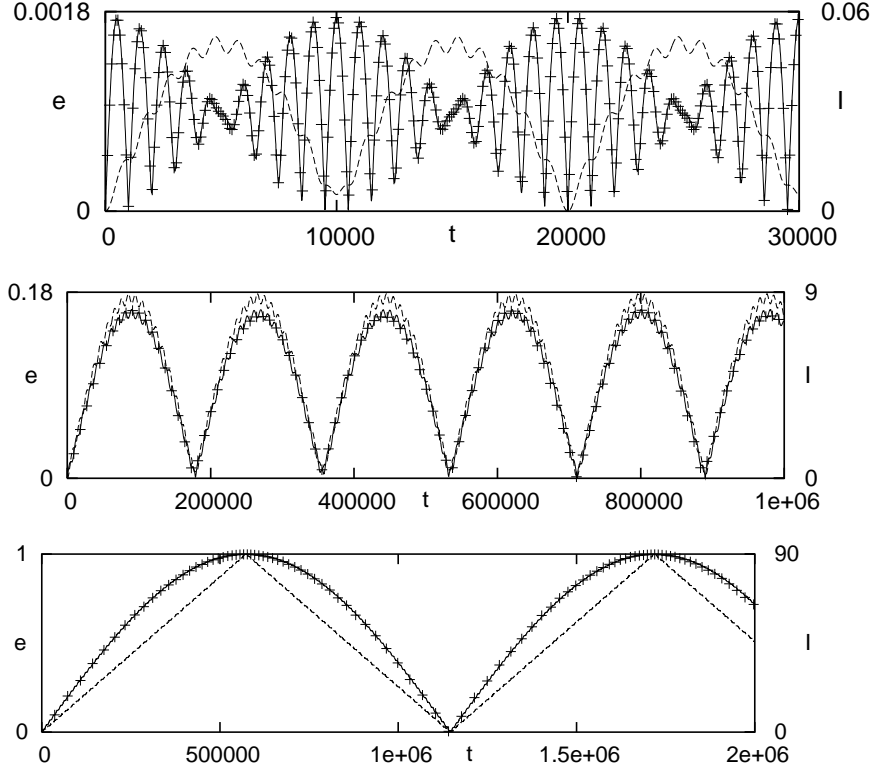


Fig. 5. Excitation of the eccentricity (solid) and inclination (dashed) by a nearly perpendicular precessing jet with an angle $\alpha = 1^\circ$. The companion's orbit is located at $a = 1$ AU and evolves from a circular orbit in a plane orthogonal to the jet's precession axis. The acceleration is $A_0 = 2 \times 10^{-10} \text{ km s}^{-2}$ yielding an excitation time of $2\pi/n_A = 10^4$ years. From top to bottom, the panels were obtained from equations (9–11) with the frequency ratios, p : 0.05, 0.9, and 1 – the precession period is $2p \times 10^4$ years. The symbols correspond to the numerical integration of the full equations of motion.

4.2 Sudden jet-induced excitation and radial migration

The location where orbits can no longer be retained by the star is where the frequency n_A becomes comparable to the local mean motion n of the companion. Near this limit, the forced periodic oscillations of the semi-major axis a are reinforced by the eccentricity and acquire large amplitudes making the orbits unstable in the long term. Calling a_{kplr} the semi-major axis of the keplerian boundary where the star where $n_A = n$, we the jet-induced acceleration is expressed as:

$$|A_0| \simeq 2 \times 10^{-12} \left(\frac{M+m}{M_\odot} \right) \left(\frac{10^3 \text{ AU}}{a_{\text{kplr}}} \right)^2 \text{ km s}^{-2} \quad (13)$$

corresponding to an excitation period $T_A = 2\pi/n_A$:

$$T_A \simeq 10^6 \left(\frac{M+m}{M_\odot} \right)^{\frac{1}{2}} \left(\frac{a_{\text{kplr}}}{10^3 \text{ AU}} \right)^2 \left(\frac{1 \text{ AU}}{a} \right)^{\frac{1}{2}} \text{ years}. \quad (14)$$

Figure (6) shows an example of an escape orbit of a constant-direction acceleration with $a_{\text{kplr}} = 10^2 \text{ AU}$ and an inclination $I_0 = 30^\circ$. The orbit's initial semi-major axis is 68.5 AU. The characteristics of motion are not strictly keplerian as the companion hovers above the star. Such escape orbits offer an interesting way to expel planets from around their parent stars or equivalently to disrupt a binary stellar system. If a companion is formed near the keplerian boundary or is pushed out to it by a possibly remaining inner disk that followed photo-evaporation [26], it could become unbound.

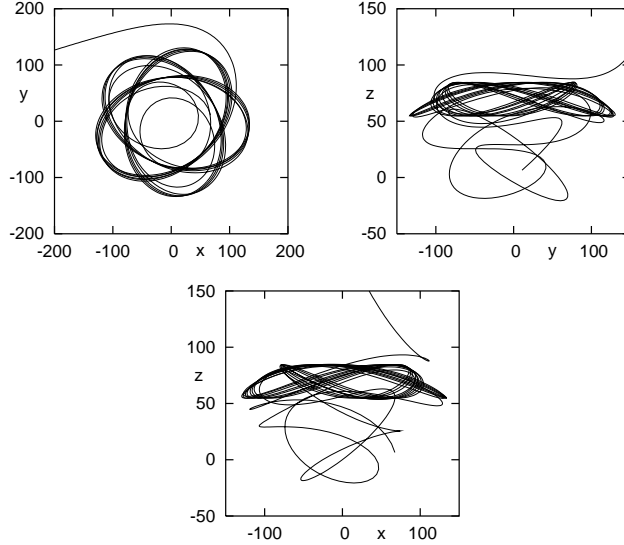


Fig. 6. Escape of a companion located near the keplerian boundary of a conservative constant-direction acceleration with $I_0 = 30^\circ$. The distances are given in AU. The boundary's semi-major axis is $a_{\text{kplr}} = 100 \text{ AU}$. Note how the companion hovers above the star before escaping.

For a realistic jet, the induced acceleration has a finite duration. Accordingly, a_{kplr} varies in time from infinity before the jet's launch to a location determined by the strongest acceleration the jet can provide. Ultimately, the keplerian boundary is pushed out to infinity. The acceleration's finite duration extends the keplerian boundary depending on the ratio of the duration τ

to the excitation time at the keplerian boundary of the equivalent constant-acceleration problem $T_A(a_{\text{kplr}})/2$. When $\tau \geq T_A(a_{\text{kplr}})/2$, orbits beyond a_{kplr} have enough time to acquire sufficient momentum and escape the gravitational pull of the star. When $\tau \leq T_A(a_{\text{kplr}})/2$, the stability region extends beyond a_{kplr} . The new stability boundary is given by the semi-major axis where $\tau \simeq T_A(a_\infty)/2$ which is larger than a_{kplr} since T_A is a decreasing function of the semi-major axis a . The expressions of T_A and the residual velocity V , show that $a_\infty \simeq G(M+m)V^{-2}$, the location where the keplerian velocity v matches V .

Orbits near the keplerian boundary of a finite duration acceleration that do not escape the pull of the star will end up with elongated orbits whose semi-major axes and eccentricity have changed. This happens because the companion feels an almost instantaneous velocity kick (the orbital period is large compared to τ). The conservation of linear momentum and energy can be combined to find the change in semi-major axis as:

$$\frac{1}{a_f} = \frac{1}{a_i} - \frac{2V \sin I_0 \cos \theta}{\sqrt{G(M+m)a_i}} - \frac{V^2}{G(M+m)}, \quad (15)$$

where a_i , a_f are the initial and final semi-major axis, θ is the longitude of the companion along its orbit, and I_0 is the inclination of the orbital plane with respect to the direction of the residual velocity \mathbf{V} . Note that for $I_0 \neq 0$, the final semi-major axis can be larger or smaller than the initial value depending on the longitude of the companion where the velocity pulse is felt.

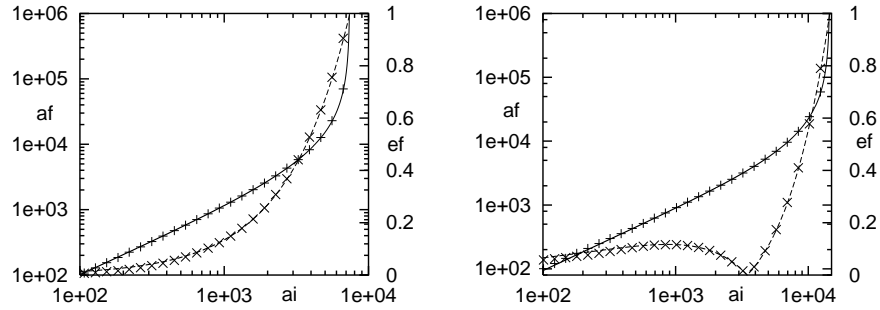


Fig. 7. Migration and eccentricity excitation near the keplerian boundary of a finite duration acceleration for two inclination values $I_0 = 0$ (left panel) and $I_0 = 20^\circ$ (right panel). In each panel, the final semi-major axis a_f (AU) (solid) and the final eccentricity e_f (dashed) are shown as a function of the initial semi-major axis a_i (AU). The parameters are: $V = 0.35 \text{ km s}^{-1}$, $a_{\text{kplr}} = 300 \text{ AU}$, and $\tau = 500$ years. The inclined circular orbits were started at the descending node ($\theta = 180^\circ$). For $I_0 = 0^\circ$, $a_\infty = 7341 \text{ AU}$ and for $I_0 = 20^\circ$, $a_\infty = 14542 \text{ AU}$.

Figure (7) shows the final semi-major axes and eccentricities at two different inclinations $I_0 = 0$ and 20° for an acceleration amplitude corresponding to

$a_{\text{kplr}} = 300$ AU and a duration $\tau = 500$ years resulting in a residual velocity $V = 0.35 \text{ km s}^{-1}$. The companions were started at the descending node for $I_0 = 20^\circ$ to illustrate inward and outward migration. Such migration could enhance the delivery of minor bodies to the Oort Cloud and explain the transport of Kuiper Belt outliers 2000 CR105 and Sedna (90377).

4.3 A test case: the ν Andromedae binary system

Multiplanet systems provide good test cases for the excitation by jet-induced acceleration. This is because mutual gravitational interactions cause the eccentricity vectors to precess. If the ensuing precession rates are much faster than the excitation frequencies, the slow build up of eccentricity by jet-induced acceleration will be lost [46, 47]. This situation is similar to that encountered for precessing jets inside the resonance radius a_{res} .

An interesting system for testing the excitation mechanism is that of ν Andromedae [3]. It contains three planets, two of which have their apsidal directions aligned [53, 33, 6] as well as a $0.2M_\odot$ stellar companion at a projected distance of 750 AU [36].

Numerical simulation can be used to reproduce the planetary orbits from initially circular co-planar orbits to their observed state [43]: $a_b = 0.059$ AU, $e_b = 0.020$, $\omega_b = 241^\circ$, $m_b \sin i = 0.75 m_J$, $a_c = 0.821$ AU, $e_c = 0.185$, $\omega_c = 214^\circ$, $m_c \sin i = 2.25 m_J$, $a_d = 2.57$ AU, $e_d = 0.269$, $\omega_d = 247^\circ$, and $m_d \sin i = 2.57 m_J$. It turns out that mutual planetary perturbations are strong enough to prevent excitation if the acceleration is smaller than $A_0 \sim 10^{-11} \text{ km s}^{-2}$. The equivalent smallest keplerian boundary is at $a_{\text{kplr}} \sim 500$ AU. Below this value, the current configuration can be recovered along with the apsidal alignment of the outer two planets. The presence of the stellar companion outside the keplerian boundary leaves us two options: either the excitation by acceleration is ruled out or that the companion was initially inside the boundary and migrated during a sudden excitation (the projected distance of 750 AU does not translate necessarily into a semi-major axis as the companion's orbit is likely to be eccentric).

Figure 8 shows a simulation of the jet-induced acceleration of the form $A(t) = A_0 / \cosh(t - t_0) / \tau$ where $A_0 \sim 3 \times 10^{-11} \text{ km s}^{-2}$ and $\tau = 2000$ years, applied the current planetary system plus a stellar companion on an orbit of semi-major axis $a = 298$ AU, just inside the keplerian boundary of A , $a_{\text{kplr}} \sim 300$ AU. The stellar companion's initial orbit was given an eccentricity $e = 0.3$ in order to decouple its perturbations from the planetary system. In particular, the eccentricity excitation by the Kozai mechanism [28] is not efficient because the corresponding excitation time ($\sim 10^7$ years) is much larger the duration of acceleration and the eccentricity secular frequency of the isolated two-planet system (~ 7000 years). The jet-induced acceleration produces a configuration similar to the observed one with stellar orbital elements: $e = 0.5$, $a = 600$ AU. Apsidal alignment is achieved as the result of the acceleration's strength that maintain the forcing of companion orbits to

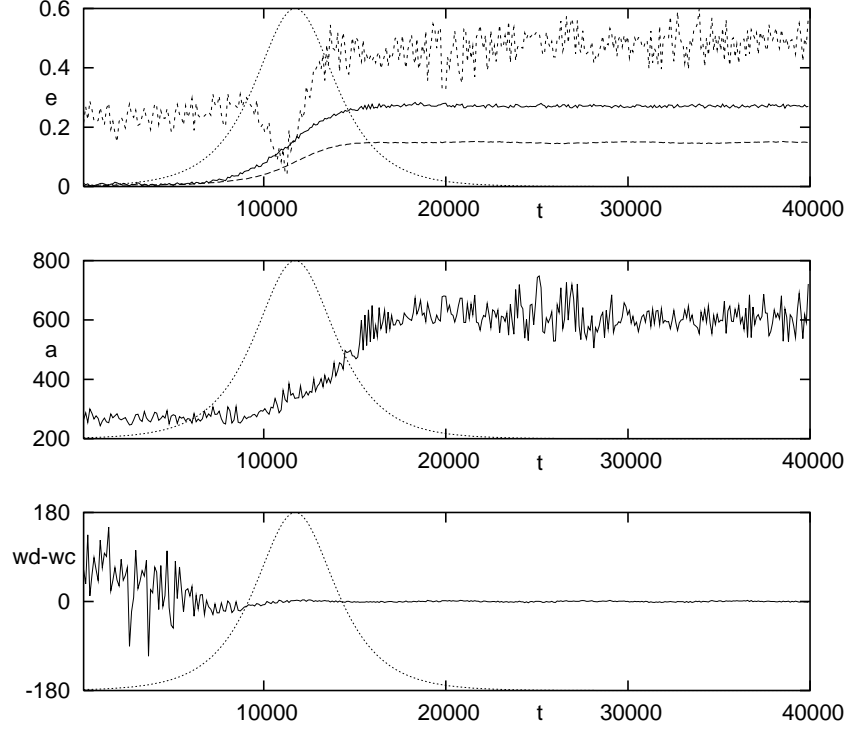


Fig. 8. Eccentricity excitation, apsidal alignment and binary migration in the v And system. The acceleration pulse is shown not to scale in all panels. The first panel shows the eccentricity excitation of planets d (solid) and c (dashed) and the eccentricity evolution of v And B (short-dashed) as well as the acceleration pulse normalized to its maximum value (dotted). The second panel shows the radial migration of v And B. The last panel shows the relative apsidal libration of planets d and c .

be perpendicular to the direction of acceleration. Note that only when the acceleration's strength is near maximum and the keplerian boundary nears 300 AU, does the stellar orbit acquire a larger eccentricity.

4.4 The solar system

Was the solar system subject to jet-induced acceleration? There are two observations that hint at the dynamical action of the solar system's jet. The first is the inclination of Jupiter's orbital normal by 6 degrees with respect to the sun's rotation axis. As Jupiter is the more massive planet in the solar system, this implies that either the early protoplanetary disk of the solar system was warped with respect to the Sun's equator plane or that the Jupiter's orbit gained inclination with respect to an early equatorial disk. Both possibilities

are consistent with the jet-induced acceleration theory. More recently, the discovery of Calcium-Aluminum inclusions in the grains of comet Wild 2 suggest that the only possibility for the Jupiter-family comet originating from the early Kuiper belt to contain such high temperature minerals is that they were transported by the solar system's jet. An additional piece of the puzzle is given by outer solar system bodies such as Sedna (90377) that are decoupled from the solar system's planets as their perihelia are larger than Neptune's orbital radius. Such objects could have been transported by the radial migration in the sudden excitation region associated with the jet-induced acceleration.

Why are the solar system's planets eccentricities small? There are three possible reasons for this: first, the resonance radius (12) where the jet's precession matches the excitation time could have been outside the planets' orbits. Inside the resonance radius, very little excitation can take place (Figure 5). Second, mutual planetary perturbations could have destroyed the secular eccentricity growth. Third, if the jet angle were to be small and the acceleration duration equally brief, the planets' location near the resonant radius would be of little help to raise their eccentricities.

4.5 The unknowns of jet-induced excitation

The unknowns of jet-induced excitation belong to two categories: (1) the unknowns of disk-planet interaction and (2) the unknowns of the time evolution of jets. In the first category comes the issue of the eccentricity damping by the accretion disk. As explained in the section about mean motion resonances, the damping of eccentricity for large eccentricity and inclination orbits is not currently understood. The advantage of jet-induced excitation with respect to the excitation during migration while in mean motion resonance is that excitation times can be much smaller than the migration timescale and the viscous timescale of the disk. In this phase, the formed planets gain a substantial inclination that makes them exit the gas disk which should in principle reduce the eccentricity damping significantly. In this context, it is useful to bear in mind that jet-induced acceleration becomes effective in a planetesimal disk only when a few planets are left. The planetesimal mutual gravitational interactions destroy excitation through the random precession of their orbits. When the bodies left in the disk are such that the precession periods due to their mutual perturbations are larger than the excitation time, jet-induced acceleration becomes effective and planets may exit the disk on inclined orbits. For the second category of unknowns, it is safe to say that except for precession, little information is available about the time variations of jets over their entire life span. Perhaps the main advantage of jet-induced excitation is its small set of parameters: amplitude, duration and jet precession frequency. These determine all the features of eccentricity growth or lack thereof. In multiplanet systems, the acceleration subjects all companions, planetary and stellar alike, to the same instability as it is independent of position and velocity. A better knowledge of the time dependence of acceleration can therefore

easily confirm or rule out the effect of jet-induced excitation in multiplanet systems.

5 Concluding remarks

The various theories of eccentricity excitation are valuable tools to gain insight into one of the most pressing if not the most pressing issue in planet formation theory: the mismatch of protoplanetary disk lifetimes and the timescales of planet formation and planet migration. Protoplanetary disk lifetimes range from 10^5 to 10^7 years. To have a viable theory, the planet formation timescale has to be smaller by at least an order of magnitude than these estimates. Planets are believed to form in two ways: (1) rocky core accretion and (2) gravitational instability. The formation of rocky cores precedes gas accumulation on the way to forming gaseous planets. This specific phase is slow. Typical formation timescales range from 10^6 to 10^7 years at Jupiter’s location [34]. Gravitational instability however has a much smaller timescale of order 10^3 years at the same location. With all its caveats about the required disk opacity for gravitational fragmentation and the role of shearing instabilities in disrupting a forming protoplanet, formation by gravitational instability looked far more promising than rocky core accretion to explain the existence of the hot Jupiters. This was true until the discovery of a hot Saturn with a 70 Earth mass rocky core orbiting the star HD 149026 [54]—for reference, the mass of Jupiter’s rocky core is believed to be 15 Earth masses. The formation of a 70 Earth mass rocky core either as a single body or as a merger of smaller cores is likely to last at least 10^7 years according to current planetesimal accumulation models. This temporal crisis does not stop at rocky core formation, it worsens because of planet migration. Migration arises from the planet’s interaction with the gas disk and has typical timescales of 10^6 years for an Earth mass core (linear regime, type I) to 10^5 years for a Jupiter mass planet (nonlinear regime, type II) [65, 9]. The duration of the eccentricity excitation phase and its dependence on the mechanism’s parameters may help elucidate the time sequence of the events that produced the observed extrasolar planets. In particular, three-dimensional hydrodynamic simulations of disk-planet interactions for eccentric and inclined orbits (off the disk’s mid-plane) may elucidate the problem of the end of resonant excitation in multiple systems. Planet-planet scattering models may benefit from including a wider mass spectrum in the populations of simulated planets. The excitation by Kozai’s secular mechanism requires further assessments of the ability to form multiple planets under the stellar companion’s perturbations [61]. Similarly, jet-induced excitation was demonstrated for a single planet under the action of a precessing acceleration. The effect of mutual planetary entrainment for planets on both sides of the precession–excitation resonance needs to be investigated and applied to observed extrasolar systems.

References

1. P. Barge, R. Pellat: *Icarus* **85**, 481 (1990)
2. P. Artymowicz: *ApJ* **419**, 166 (1993)
3. R.P. Butler, G.W. Marcy, E. Williams, H. Hauser, P. Shirts: *ApJ* **474**, L115 (1997)
4. S. Chandrasekhar: *Principles of stellar dynamics* (The University of Chicago press, Chicago, 1942)
5. G. Chauvin, A.M. Lagrange, C. Dumas, B. Zuckerman, D. Mouillet, I. Song, J.L. Beuzit, P. Lowrance: *AA* **438**, L25 (2005)
6. E.I. Chiang, S. Tabachnik, S. Tremaine: *AJ* **122**, 1607 (2001)
7. E.I. Chiang, D. Fischer, E. Thommes: *ApJ* **564**, L105 (2002)
8. A. Cotera, B.A. Whitney, E. Young, M.J. Wolff, K. Wood, M. Povich, G. Schneider, M. Rieke, R. Thompson: *ApJ* **556**, 958 (2001)
9. G. D'Angelo, W. Kley, T. Henning: *ApJ* **586**, 540 (2003)
10. C.J. Davis, J. Eislöffel, T.P. Ray, T. Jenness: *AA* **324**, 1013 (1997)
11. J. Eislöffel, M.D. Smith, C.J. Davis, T.P. Ray: *AJ* **112**, 2086 (1996)
12. J. Eislöffel, R. Mundt, T.P. Ray, L.F. Rodríguez: In *Protostars and Planets IV* ed by V. Mannings, A.P. Boss, S.S. Russel (University of Arizona Press, Tucson 2000) pp 815
13. M. Fernández, F. Comerón: *AA* **440**, 1119 (2005)
14. E.B. Ford, B. Kozinsky, F.A. Rasio: *ApJ* **535**, 385 (2000)
15. E.B. Ford, M. Havlickova, F.A. Rasio: *Icarus* **150**, 303 (2001)
16. E.B. Ford, F.A. Rasio, K. Yu: In *ASP conf series*, vol 294, ed by D. Deming, S. Seager (ASP, San Francisco 2003) pp 181-188
17. P. Goldreich, S. Tremaine: *ApJ* **233**, 857 (1979)
18. P. Goldreich, S. Tremaine: *ApJ* **241**, 425 (1980)
19. P. Goldreich, S. Tremaine: *ApJ* **243**, 1062 (1981)
20. P. Goldreich, R. Sari: *ApJ* **585**, 1024 (2003)
21. J.L. Halbwachs, M. Mayor, S. Udry: *AA* **431**, 1129 (2005)
22. P. Hartigan, S. Edwards, R. Pierson: *ApJ* **452**, 736 (1995)
23. P. Hartigan, J. Mundt, B. Reipurth, J.A. Morse: In *Protostars and Planets IV* ed by V. Mannings, A. Boss, S.S. Russel (University of Arizona Press, Tucson 2000) pp 841
24. G.A. Hirth, R. Mundt, J. Solf: *ApJ*, **427**, L99 (1994)
25. D. Hollenbach: *Icarus* **61**, 36 (1985)
26. D.J. Hollenbach, H.W. Yorke, D. Johnston: In *Protostars and Planets IV* ed by V. Mannings, A. Boss, S.S. Russel (University of Arizona Press, Tucson 2000) pp 401
27. M. Holman, J. Touma, S. Tremaine: *Nature* **386**, 254 (1997)
28. Y. Kozai: *AJ* **67**, 591 (1962)
29. J. Kwan, E. Tademaru: *ApJ* **454**, 382 (1995)
30. C. Lavalley, S. Cabarit, c. Dougados, P. Ferruit, R. Bacon: *AA* **327**, 671 (1997)
31. M.H. Lee, S.J. Peale: *ApJ* **567**, 596 (2002)
32. D.N.C. Lin, J.C.B. Papaloizou: *MNRAS* **186**, 799 (1979)
33. J.J. Lissauer, E.J. Rivera: *ApJ* **554**, 1141 (2001)
34. J.J. Lissauer, D.J. Stevenson: In *Protostars and Planets V* ed by B. Reipurth, D. Jewitt, K. Keil (University of Arizona Press, Tucson 2006), in press
35. L. López-Martín, S. Cabrit, C. Dougados, *AA* **405**, L1 (2003)

36. P.J. Lowrance, J.D. Kirkpatrick, C.A. Beichman: *ApJ* **572**, L79 (2002)
37. S. Lubow, G. Ogilvie: *ApJ* **587**, 398 (2003)
38. F.S. Masset, G.I. Ogilvie: *ApJ* **615**, 1000 (2004)
39. F.S. Masset, M. Snellgrove : *MNRAS* **320**, L55 (2001)
40. F. Marzari, S. Weidenschilling: *Icarus* **156**, 570 (2002)
41. M. Mayor, D. Queloz: *Nature* **378**, 355 (1995)
42. T. Mazeh, Y. Krymolowski, G. Rosenfeld: *ApJ* **477**, L103 (1997)
43. D. Naef, M. Mayor, J.L. Beuzit, C. Perrier, D. Queloz, J.P. Sivan, S. Udry: *AA* **414**, 351 (2002)
44. F. Namouni, J.F. Luciani, R. Pellat: *AA* **307**, 972 (1996)
45. F. Namouni: *MNRAS* **300**, 915 (1998)
46. F. Namouni: *AJ* **130**, 280 (2005)
47. F. Namouni, J.L. Zhou: *CMDA* **95**, 245 (2006)
48. J.C.B. Papaloizou, C. Terquem: *MNRAS* **274**, 987 (1995)
49. J.C.B. Papaloizou, C. Terquem: *MNRAS* **325**, 221 (2001)
50. S.J. Peale: *ARAA* **37**, 533 (1999)
51. F. Pepe, M. Mayor, F. Galland, D. Naef, D. Queloz, N.C. Santos, S. Udry, M. Burnet: *AA* **388**, 632 (2002)
52. F. Rasio, E. Ford: *Science* **274**, 954 (1996)
53. E.J. Rivera, J.J. Lissauer: *ApJ* **530**, 454 (2001)
54. B. Sato, and 20 co-authors: *ApJ* **633**, 465 (2005)
55. J. Schneider: <http://www.obspm.fr/planets> (1996)
56. K. R. Stapelfeldt and 15 co-authors: *ApJ* **516**, L95 (1999)
57. T.F. Stepinski, D.C. Black: *AA* **371**, 250 (2001)
58. G. Takeda, F.A. Rasio: *ApJ* **512**, 1001 (2005)
59. C. Terquem, J. Eislöffel, J.C.B. Papaloizou, R.P. Nelson : *ApJ* **512**, L131 (1999)
60. C. Terquem, J.C.B. Papaloizou: *MNRAS* **332**, L39 (2002)
61. P. Thébault, F. Marzari, H. Scholl, D. Turrini, M. Barbieri: *AA* **427**, 1097 (2004)
62. K. Tsiganis, R. Gomes, A. Morbidelli, H.F. Levison: *Nature* **435**, 459 (2005)
63. S. Udry, M. Mayor, D. Naef, F. Pepe, D. Queloz, N.C. Santos, M. Burnet, B. Confino, C. Melo: *AA* **356**, 590 (2000)
64. W.R. Ward: *Icarus* **73**, 330 (1988)
65. W.R. Ward, J.M. Hahn: In *Protostars and Planets IV* ed by V. Mannings, A. Boss, S.S. Russel (University of Arizona Press, Tucson 2000) pp 1135
66. A.M. Watson, K.R. Stapelfeldt, J.E. Krist, C.J. Burrows: *BAAS* **32**, 1481 (2000)
67. S. Weidenschilling, F. Marzari: *Nature* **384**, 619 (1996)
68. J. Wisdom: *AJ* **85**, 1122 (1980)
69. A. Wolszczan, D.A. Frail: *Nature* **355**, 145 (1992)
70. Q. Yu, S. Tremaine: *AJ* **121**, 1736 (2001)
71. N. Zakamska, S. Tremaine: *AJ* **128**, 869 (2004)